PHYSICAL REVIEW A VOLUME 17, NUMBER 5 MAY 1978

Relation between the equilibrium and nonequilibrium critical properties of the Dicke model

R. Gilmore
Physics Department, University of South Florida, Tampa, Florida 33620

L. M. Narducci
Department of Physics and Atmospheric Science, Drexel University, Philadelphia, Pennsylvania 19104

(Received 12 May 1977)

The connection between the critical properties of the Dicke model, subject to equilibrium and nonequilibrium boundary conditions, is explicitly exhibited. The Langevin equations generated by the Dicke Hamiltonian lead to a single nonlinear order-parameter equation that characterizes the stationary states of the system. We prove the existence of two essentially identical manifolds of stationary states, one for equilibrium, the other for nonequilibrium boundary conditions. These manifolds can each be derived from a potential obtained from the nonlinear order-parameter equations. In the equilibrium case the potential is the free energy of the system; in the nonequilibrium case it can be identified with the so-called "laser potential." The reduced-density operator for the field and atomic subsystems factors into a geometric and a physical part. The geometric part is determined by the system signal; the physical part, by the system noise. This is exhibited explicitly with an example taken from the theory of photoelectron counting. The identification of the stationary-state manifolds for the Dicke model subject to equilibrium and nonequilibrium conditions with the same geometric (cusp) manifold allows a real analytic continuation of model properties from the equilibrium configuration to the nonequilibrium dissipative regime. Three types of stability are considered: static, dynamical, and structural. Structural-stability considerations lead to strong conclusions about the effects of additional perturbations on the Dicke model.

I. INTRODUCTION

The Dicke-model Hamiltonian[1] has been studied extensively subject to both equilibrium and nonequilibrium boundary conditions.

Under nonequilibrium boundary conditions, this Hamiltonian provides a reasonable model for the working of a single-mode laser.[2] As the atomic system is pumped, the population inversion increases. For sufficiently large population inversion, the system may undergo a second-order phase transition[3] from a disordered state with a small number of photons and $\langle a\rangle = 0$ ($\langle a\rangle$ is the expectation value of the electric field lowering operator) to an ordered state with a large number of photons, displaying coherence ($\langle a\rangle \neq 0$).

Under equilibrium boundary conditions, this Hamiltonian provides an exactly soluble model exhibiting a second-order phase transition in the thermodynamic limit.[4] At a sufficiently low temperature, the system may undergo a second-order phase transition from a disordered state with a small number of photons and $\langle a\rangle = 0$ to an ordered state with a large number of photons displaying coherence. Conditions for the existence of the second-order phase transitions under equilibrium and nonequilibrium boundary conditions are strikingly similar. [See Eq. (9.1).]

Recent interest in the Dicke model has focused on the effects of external perturbations, such as the classical resonant electric field responsible for optical bistability.[5] Under equilibrium boundary conditions, the second-order phase transition is unstable. For a fixed nonzero external field, the second-order transition as a function of decreasing temperature disappears.[6] In its place, a first-order phase transition may be observed if the system is first taken below the critical temperature, and if the field is then made sufficiently large (see Fig. 2).

Under nonequilibrium boundary conditions, the second-order phase transition is also unstable. For fixed nonzero external field, the second-order phase transition as a function of increasing population inversion disappears (see Fig. 3). In its place a first-order phase transition may be observed when the system is held below threshold for laser action and the external field is increased, subject to appropriate conditions.[7]

These behavioral similarities are not at all accidental, but come from underlying geometrical similarities. We exhibit this identification below.

In Sec. II, we derive the Langevin equations for the Dicke model in the mean-field approximation. The stationary states are determined in Sec. III by combining the three coupled nonlinear equations for the operator expectation values $\langle a\rangle, \langle \sigma^{-}\rangle, \langle \sigma^{z}\rangle$ into a single nonlinear equation for $\langle a\rangle$. This equation is essentially a cubic equation under both equilibrium and nonequilibrium boundary conditions. Therefore, it can be identified with the canonical form for such equations, the so-called

"cusp catastrophe" manifold.[8] This is done in Sec. IV. The manifold of stationary states is shown in Fig. 1. The effects of varying temperature and external electric field under equilibrium boundary conditions are shown in Fig. 2. In Fig. 3, we describe the effects of varying the population inversion and the external electric field under nonequilibrium boundary conditions. All the behavior characteristics described above can be determined at a glance from these three figures.

In Sec. V, we derive the potential functions governing the system under each boundary condition. These potentials are obtained by integrating the equations for the manifold of stationary states (3.3). Under equilibrium conditions, the potential is just the free energy, previously known in the limit of zero injected external field. Under nonequilibrium conditions, it is just the laser potential.[3] This potential is not a free energy, although it is customary to refer to it as such. In Sec. VI, we discuss the main features of optical bistability in the light of our analysis of nonequilibrium systems. The observed behavior of the transmitted light intensity[9] becomes especially transparent when interpreted in terms of the steady-state trajectories displayed in Fig. 3.

In Sec. VII, we compute the system density operators. Under mean-field assumptions, the density operator factors into the direct product of reduced-density operators, one for the field subsystem, the other for the atomic subsystem. Both the field and atomic reduced-density operators, under equilibrium and nonequilibrium boundary conditions, with both zero and nonzero field, factor in the sense implied by the following equation:

$$\rho = [\rho(\text{geometry})]^{M(\text{physics})} . \tag{1.1}$$

Here, ρ(geometry) is an operator defined on the manifold of stationary states, and the number M(physics) depends upon physical conditions. In the case of photon-counting experiments,[10] for example, ρ(geometry) is determined by the system signal only, while M(physics) is assigned by the system noise.

The correspondence between points on the cusp manifold and the density operators describing the equilibrium states of the system suggests the possibility of an "analytic continuation" from equilibrium to nonequilibrium configurations. The term "analytic continuation" is introduced here not in the usual sense of complex variables, but rather in the sense of real differential geometry. This procedure may provide a powerful tool for the analysis of nonequilibrium properties simply from a knowledge of the equilibrium behavior.

Three types of stability are discussed in Sec. VIII: static, dynamic, and structural. From the analysis of the latter, we learn that no essentially new types of steady-state behavior can be expected in this model by introducing additional perturbations. The only effect induced by these perturbations is a modification of the steady-state trajectories, such as that shown in Figs. 2 and 3. The structure of the stationary manifold remains unchanged under perturbation.

The physical implications of the Langevin equations are explored in Sec. IX. In the Appendix, we extend the semiclassical theorem[11] from generalized coherent states to Gibbs states.

Throughout, we use the notations $\beta = 1/kT$, E and N for equilibrium and nonequilibrium boundary conditions, and i and ii to distinguish the two cases: zero external field, nonzero external field.

II. LANGEVIN EQUATIONS

The Hamiltonian considered in this work is

$$H = H_D + H_B . \tag{2.1}$$

Here H_D is the single-mode Dicke Hamiltonian in the long-wavelength approximation[1] including the interaction energy due to a classical external field,

$$H_D = \omega a^\dagger a + \epsilon \sum_{j=1}^{N} \frac{1}{2} \sigma_j^z + \frac{1}{\sqrt{N}} \sum_{j=1}^{N} [\lambda (a^\dagger + \alpha^* \sqrt{N}) \sigma_j^- + \lambda^* (a + \alpha \sqrt{N}) \sigma_j^+] . \tag{2.2}$$

The rotating-wave approximation has been made, and the $\vec{A} \cdot \vec{A}$ term ($\vec{A}$ is the field vector potential) has been temporarily neglected. The Hamiltonian H_B describes the interaction of each atom and of the field mode with external heat baths and with external driving sources (fields and currents). For the equilibrium and nonequilibrium boundary conditions described in the work, $H_B \neq 0$. For laser operation, $\omega \approx \epsilon$.

The equations of motion for the operators are the familiar Heisenberg equations of motion ($\hbar = 1$)

$$i \frac{d\theta}{dt} = [\theta, H_D] + [\theta, H_B] . \tag{2.3}$$

The first term on the right-hand side of Eq. (2.3) can be computed explicitly using Eq. (2.2). The second term is responsible for two effects. One is to introduce a stochastic forcing term $\Gamma_\theta(t)$, with zero expectation value, into each equation of motion.[12] The second effect is to force regression of fluctuations of operator expectation values back to time-independent values. For example, if $\delta\theta$ is a fluctuation of $\langle\theta\rangle$ from its time-independent value $\langle\theta\rangle_\infty$, then interaction with the bath forces a decay of $\langle\theta\rangle(t)$ in the following phenomenological way:

$$\langle\theta\rangle = \delta\theta\, e^{-\gamma_\theta t} + \langle\theta\rangle_\infty \ .$$

The action of the bath can be taken into account by replacing the operator equation (2.3) with the phenomenological equation for the expectation values,

$$i\left(\frac{d}{dt}+\gamma_\theta\right)(\langle\theta\rangle - \langle\theta\rangle_\infty) = \langle[\theta, H_D]\rangle + \langle\Gamma_\theta(t)\rangle \ .$$

In addition, it is customary[3,12] to assume that $\langle\Gamma_\theta(t)\rangle = 0$. Here, $\langle\theta\rangle_\infty$ is to be interpreted as the time-independent $(d/dt \to 0)$ expectation value that $\langle\theta\rangle$ would have in the limit of *very fast* relaxation (i.e., $\gamma_\theta \to \infty$).

The expectation values of the operators appearing in the Dicke model (2,2) then satisfy the phenomenological equations of motion

$$\begin{aligned}
&i\left(\frac{d}{dt}+\kappa\right)(\langle a\rangle - \langle a\rangle_e) = \omega\langle a\rangle + \lambda\sqrt{N}\langle\sigma^-\rangle \ ,\\
&i\left(\frac{d}{dt}+\gamma_\perp\right)(\langle\sigma^-\rangle - \langle\sigma^-\rangle_e)\\
&\qquad = \omega\langle\sigma^-\rangle - \frac{\lambda^*}{\sqrt{N}}\langle(a+\alpha\sqrt{N})\sigma^z\rangle \ , \qquad (2.4)\\
&i\left(\frac{d}{dt}+\gamma_\parallel\right)(\langle\sigma^z\rangle - \langle\sigma^z\rangle_e)\\
&\qquad = -2\frac{\lambda}{\sqrt{N}}\langle(a^\dagger+\alpha^*\sqrt{N})\sigma^-\rangle + 2\frac{\lambda^*}{\sqrt{N}}\langle(a+\alpha\sqrt{N})\sigma^+\rangle,\\
&i\left(\frac{d}{dt}+\gamma_n\right)(\langle a^\dagger a\rangle - \langle a^\dagger a\rangle_e)\\
&\qquad = \omega\lambda\sqrt{N}\langle a^\dagger\sigma^-\rangle - \omega\lambda^*\sqrt{N}\langle a\sigma^+\rangle \ ,
\end{aligned}$$

where κ, $\gamma_\perp$, $\gamma_\parallel$, and γ_n are the relaxation rates of the respective dynamical variables.

Equations (2.4) are intractable in their present form. They are simplified by assuming that, for large number of atoms, each subsystem (atom, field) behaves in a stochastically uncorrelated way with respect to the other. This is equivalent to a mean-field approximation, or to the assumption that the density operator factors into the form $\rho = \rho_F \otimes \rho_A$, where ρ_F describes the field subsystem alone, and ρ_A the atomic subsystem.

With these assumptions the operator expectation values in Eq. (2.4) factor. Next, we introduce the convenient notations

$$\begin{aligned}
&\mu = \langle a\rangle/\sqrt{N} = \langle a^\dagger\rangle^*/\sqrt{N} \ ,\\
&\nu = \langle\sigma^-\rangle = \langle\sigma^+\rangle^* \ ,\\
&\sigma = \langle\sigma^z\rangle \ ,\\
&n = \langle a^\dagger a\rangle/N \ .
\end{aligned} \qquad (2.5)$$

After the mean-field approximation, the system (2.4) reduces, in the notation of (2.5), to the more tractable system

$$\begin{aligned}
&i\left(\frac{d}{dt}+\kappa\right)(\mu-\mu_\infty) = \omega\mu + \lambda\nu \ ,\\
&i\left(\frac{d}{dt}+\gamma_\perp\right)(\nu-\nu_\infty) = \epsilon\nu - \lambda^*(\mu+\alpha)\sigma \ ,\\
&i\left(\frac{d}{dt}+\gamma_\parallel\right)(\sigma-\sigma_\infty) = -2\lambda(\mu+\alpha)^*\nu + 2\lambda^*(\mu+\alpha)\nu^* \ ,\\
&i\left(\frac{d}{dt}+\gamma_n\right)(n-n_\infty) = \omega\lambda\mu^*\nu - \omega\lambda^*\mu\nu^* \ .
\end{aligned} \qquad (2.6)$$

In what follows we assume λ to be real and α to be real and positive.

The equations governing the two regimes discussed in Sec. I are now easily obtained from Eqs. (2.6).

Equilibrium

Under equilibrium boundary conditions, the left-hand side of each of Eqs. (2.6) is zero. All operator expectation values assume their thermal equilibrium values, denoted by the subscript e:

$$\begin{aligned}
&0 = \omega\mu_e + \lambda\nu_e \ ,\\
&0 = \omega\nu_e - \lambda(\mu_e+\alpha)\sigma_e \ ,
\end{aligned} \qquad (2.7\text{E})$$

where

$$\begin{aligned}
&\sigma_e = -(\omega/2\theta)\tanh\beta\theta,\\
&\theta^2 = (\tfrac{1}{2}\epsilon)^2 + \lambda^2|\mu_e+\alpha|^2 \ .
\end{aligned}$$

Here σ_e is computed in a self-consistent way from Eq. (2.2) by taking the trace of the operator σ^2 multiplied by the equilibrium density operator.[13] The coupled nonlinear equations (2.7E) have been used to describe the Dicke model in thermodynamic equilibrium.[13]

Nonequilibrium

In the case of nonequilibrium boundary conditions, the fast time dependence of $\langle a\rangle$ and $\langle\sigma^-\rangle$ is first removed by means of the substitutions $\mu(t) = \tilde{\mu}(t)e^{-i\omega t}$, $\nu(t) = \tilde{\nu}(t)e^{-i\epsilon t}$, and similarly for $\mu_\infty(t)$, $\nu_\infty(t)$. The steady-state nonequilibrium equations are obtained by setting the time derivatives of the envelopes $\tilde{\mu}(t)$, $\tilde{\nu}(t)$ equal to zero. It is customary to assume that the expectation values $\tilde{\mu}_\infty$, $\tilde{\nu}_\infty$ vanish.[12] Finally, dropping the tilde for notational convenience, the steady-state expectation values (denoted by a subscript s) are

$$\begin{aligned}
&i\kappa\mu_s = \lambda\nu_s \ ,\\
&i\gamma_\perp\nu_s = -\lambda(\mu_s+\alpha)\sigma_s \ ,\\
&i\gamma_\parallel(\sigma_s-\sigma_e) = -2\lambda(\mu_s+\alpha)^*\nu_s + 2\lambda(\mu_s+\alpha)\nu_s^* \ .
\end{aligned} \qquad (2.7\text{N})$$

Equations (2.7N) have been used[2,12] to describe the steady-state behavior of the single-mode laser

($\alpha = 0$) and the bistable behavior[7] observed[9] in optical experiments ($\alpha \neq 0$).

III. STATIONARY NONLINEAR EQUATIONS

It is useful to study Eqs. (2.7E) and (2.7N) by eliminating ν and σ and constructing a single nonlinear equation for the order parameter μ. The resulting equations are[14]

$$\epsilon\omega\mu_e - (\lambda^2\epsilon/2\theta)(\mu_e + \alpha)\tanh\beta\theta = 0\,, \tag{3.1E}$$

$$\kappa\gamma_\perp\alpha + (\lambda^2\sigma_\infty - \kappa\gamma_\perp)(\mu_s + \alpha) - (4\kappa/\gamma_\parallel)\lambda^2(\mu_s + \alpha)^2\mu_s = 0\,. \tag{3.1N}$$

In deriving (3.1N) we have used the assumption that μ and α are real.

IV. STATIONARY MANIFOLD

The nonlinear equations (3.1) are essentially cubics. Hence they can be studied conveniently in terms of the geometry of the A_3 or "cusp catastrophe."[15,16] Given the potential

$$V(x;A,B) = \tfrac{1}{4}x^4 - \tfrac{1}{2}Ax^2 - Bx\,, \tag{4.1}$$

the set of equilibrium points $dV/dx = 0$ is the two-dimensional manifold

$$x^3 - Ax - B = 0 \tag{4.2}$$

in the three-dimensional space with coordinates x; A, B. (See Fig. 1.) Inside the cusp-shaped region in the AB plane with boundary $(\frac{1}{3}A)^3 = (\frac{1}{2}B)^2$, Eq. (4.2) has three solutions, two corresponding to a local minimum of V, one to a local maximum. On the cusp boundary, the local maximum coalesces with one of the local minima, and outside this region the manifold is single valued.

The four physical situations described in Sec. I are studied from a unified viewpoint by identifying the appropriate forms of Eqs. (3.1) with the cusp manifold (4.2). For this purpose, we identify the state parameter x with a linear function of the order parameter $\mu_s = \langle a\rangle/\sqrt{N}$, and the control parameters A and B with appropriate combinations of the physical constants, temperature and field (α) for equilibrium boundary conditions, equilibrium population inversion (σ_∞) and field (α) for nonequilibrium boundary conditions. A variation of the physical parameters defines a trajectory in control parameter space (AB plane in Fig. 1); this is then "lifted" to the cusp manifold to determine the trajectory of the state parameter.

Equilibrium

The equilibrium manifold (3.1E) looks qualitatively like the cusp manifold of Fig. 1. The identification of Eq. (3.1E) with the canonical form (4.2) is made precise by letting $x = \mu_e + \alpha$, expanding the hyperbolic tangent for small values of x, and discarding terms of degree higher than third. In this limiting case,[17] we find

$$x = \mu_e + \alpha\,,$$
$$A = -(1/C)[\epsilon\omega - \lambda^2\tanh(\tfrac{1}{2}\beta\epsilon)]\,, \tag{4.3E}$$
$$B = \epsilon\omega\alpha/C\,,$$

where

$$C = 2(\lambda^2/\epsilon)^2[\tanh(\tfrac{1}{2}\beta\epsilon) - \tfrac{1}{2}\beta\epsilon\,\mathrm{sech}^2(\tfrac{1}{2}\beta\epsilon)]\,.$$

The parameter C is positive for $T < \infty$. The physical control parameters, as indicated before, are the temperature and the external field.

Case i. In the absence of an external field, the parameter B is identically zero. If $\lambda^2/\epsilon\omega < 1$, A is negative for all temperatures. It is clear that the trajectory never reaches the cusp point and that the stationary solution for μ_e is unique and equal to zero throughout (disordered state).

If $\lambda^2/\omega\epsilon > 1$, the trajectory passes through the cusp point at the critical temperature T_c defined by the condition $1 = (\lambda^2/\epsilon\omega)\tanh(\frac{1}{2}\beta_c\epsilon)$. A bifurcation from the disordered state $\mu_e = 0$ to the ordered state $\mu_e \neq 0$ occurs at $\beta = \beta_c$. The equations for the stationary values do not determine which of the two stable sheets in Fig. 1 the solution travels on

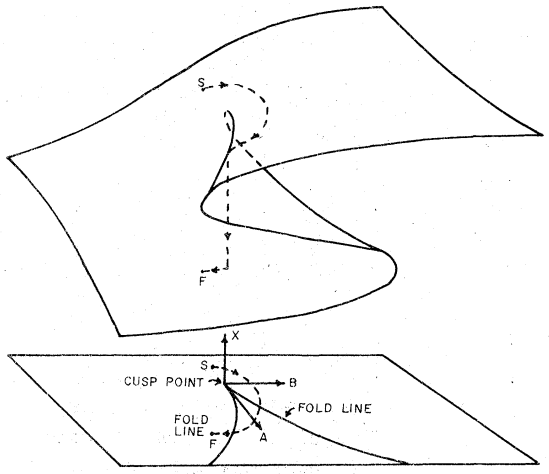

FIG. 1. The surface $x^3 - Ax - B = 0$ is a two-dimensional pleated manifold in the three-dimensional space with coordinates $(x; A, B)$. Outside the cusp-shaped region in the central plane AB bounded by the fold lines $(\frac{1}{3})^3 = (\frac{1}{2})^2$, the surface is single valued; inside, it is triple valued. When the control-parameter trajectory follows the continuous dashed path in the AB plane, starting at s and ending at f, the system-state parameter x undergoes discontinuous behavior when crossing the second fold line. This is clear when the trajectory is lifted from the AB plane to the cusp manifold above.

for $T < T_c$.

Case ii. For $\alpha > 0$, the control parameter B is also positive and the trajectory, for decreasing temperature and fixed α, passes to the right of the cusp point. There is no bifurcation,[18] and the state parameter x passes continuously onto the upper sheet. The effects of changing the temperature and external field on the control parameters A and B, and hence the state parameter x, are summarized in Fig. 2. The disappearance of the second-order phase transition is simply a manifestation of the structural instability of the zero-field Dicke model,[18] or, more generally, a feature of the $B = 0$ cusp catastrophe[19] under arbitrarily small symmetry-breaking perturbations.

Nonequilibrium

The nonequilibrium steady-state manifold (3.1N) can be cast into the canonical form (4.2) for the cusp catastrophe manifold through the identifications

$$x = \mu_s + \tfrac{2}{3}\alpha\,,$$
$$A = \frac{\alpha^2}{3} + \frac{\gamma_\parallel}{4\kappa}\left(\sigma_e - \frac{\gamma_\perp \kappa}{\lambda^2}\right), \tag{4.3N}$$
$$B = \frac{2\alpha^3}{27} + \frac{\alpha}{3}\,\frac{\gamma_\parallel}{4\kappa}\left(\sigma_e - \frac{\gamma_\perp \kappa}{\lambda^2}\right) + \frac{\gamma_\perp \gamma_\parallel}{4\lambda^2}\,\alpha\,.$$

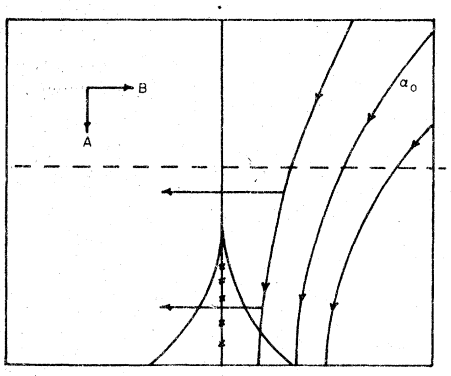

FIG. 2. Under equilibrium conditions the manifold of stationary states (4.3) looks like (is "diffeomorphic to" (Ref. 15) the cusp manifold of Fig. 1. This identification is made in Eq. (4.4). The parameter B is always positive when α is positive. In the high temperature limit, we have $\mu_e \to 0$, $x \to \alpha$, and $B/(-A) \to \alpha$. Trajectories are plotted for various values of α and decreasing temperature. The trajectories terminate at $T = 0$ with the maximum value of A, which is negative (dashed line) for $\lambda^2/\epsilon\omega < 1$ and positive (bottom edge) for $\lambda^2/\epsilon\omega > 1$. For $\lambda^2/\epsilon\omega > 1$ and $\alpha = 0$ the trajectory passes through the cusp point for $A = \epsilon\omega - \lambda^2 \tanh\frac{1}{2}\beta_c \epsilon = 0$. For lower temperatures, it passes to the upper or lower sheet (crosses) in a second-order phase transition. For $\alpha > 0$, the trajectory passes to the right of the cusp and moves continuously onto the upper sheet of the cusp manifold. For $\alpha < \alpha_0 = \lambda/2\omega\,[1-(\epsilon\omega/\lambda^2)^{2/3}]^{3/2}$ the trajectory enters the cusp region (on the upper sheet). For $\alpha > \alpha_0$, it does not. When the field is reversed and made sufficiently negative, the system may or may not experience a first-order phase transition depending on whether T is below or above the critical temperature. This phenomenon is represented by the horizontal arrows to the left and is known as "divergence".

Case i. In the absence of an applied external field, the parameter B is identically zero. As in the case of equilibrium boundary conditions, we distinguish two situations. If $\lambda^2/\kappa\gamma_\perp < 1$, A is negative for all values of σ_e and the trajectory in control-parameter space terminates with the maximum value of A (which is negative) as σ_e approaches unity. The trajectory never reaches the cusp point and the only stationary solution for μ_s is unique and equal to zero (disordered state).

If $\lambda^2/\kappa\gamma_\perp > 1$, the trajectory passes through the cusp point at the critical population inversion σ_c defined by $1 = \lambda^2\sigma_\infty/\gamma_\perp\kappa$. A bifurcation from the disordered state $\mu_s = 0$ to the ordered state $\mu_s \neq 0$ occurs at $\sigma_\infty = \sigma_c$. The equation for the stationary value does not determine which of the two stable sheets in Fig. 1 the solution travels on for $\sigma_\infty > \sigma_c$.

Case ii. In the recent experimental work on optical bistability,[9] the atomic system is held below threshold in the sense that $A(\alpha = 0) < 0$. Typical trajectories in control-parameter space are shown for increasing value of α and fixed σ_∞ in Fig. 3. The system begins, for $\alpha = 0$, in the single-sheeted regime and passes continuously onto the upper sheet as the trajectory passes to the right of the cusp point. If the trajectory passes to the left of the cusp, the system state lies on the lower sheet and remains there until the right-hand fold line is crossed (delay convention).[16] At this point, the system passes discontinuously to the upper sheet. For decreasing α, the system state remains on the upper sheet as long as possible. When the left-hand fold line is crossed, the state parameter jumps "catastrophically" to the lower sheet. The system exhibits bistable behavior, hysteresis, discontinuous jumps, and divergence.

The trajectory (separatrix) which passes through the cusp point is characterized by the condition

$$-\sigma_\infty = 8\gamma_\perp\kappa/\lambda^2\,. \tag{4.4}$$

A first-order phase transition occurs for

$$\lambda^2(-\sigma_\infty)/8\gamma_\perp\kappa > 1\,. \tag{4.5}$$

If the inequality (4.5) is reversed, the system evolves continuously along a line of equilibrium states.

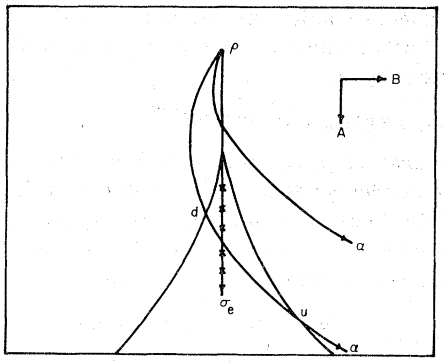

FIG. 3. For $\alpha = 0$ the coordinates of the point P are $B = 0$, $A = (\gamma_\parallel/4\kappa)(\sigma_e - \gamma_\perp\kappa/\lambda^2)$. As σ_e is increased from -1 to $+1$, corresponding to increased pumping of the atomic subsystems, the trajectory of the point P passes through the cusp point $A = [\sigma_e - (\gamma_\perp\kappa/\lambda^2)] = 0$. For higher population inversion it passes to the upper or lower sheet (crosses) in a second-order phase transition. The tangent to the trajectory at $\alpha = 0$ (point P) rotates in the counterclockwise direction as σ_e approaches σ_c from below, and points into the lower right quadrant at $\sigma_e = \sigma_c$. For $\alpha > 0$, the system state passes automatically onto the upper sheet as σ_e is increased above threshold. No phase transition occurs. The two curved trajectories shown in the figure are for fixed σ_e below threshold, with α increasing from 0. The qualitative behavior of the system depends on the ratio $Q = 8\gamma_\perp\kappa/\lambda^2(-\sigma_e)$. The trajectory for $Q = 1$ (not shown) passes through the cusp and acts as a separatrix. For $Q < 1$ the trajectory passes to the right of the cusp, and no phase transition occurs. For $Q > 1$, the trajectory curves to the left of the cusp, passes continuously onto the lower sheet and remains there as α is increased until point u is reached. The system state then jumps discontinuously onto the upper sheet. For α decreasing, the state parameter x remains tied to the upper sheet until the other fold is crossed at d. In this way bistability and hysteresis occur, and divergence ($Q < 1$, $Q > 1$) is exhibited. First-order phase transitions occur at the fold curves assuming the delay convention. The lines of first-order phase transitions terminate as $Q = 1$, $\alpha^2 = (-\sigma_e)(\gamma_\parallel/4\kappa)(\frac{3}{2})^3$.

V. POTENTIALS

The surfaces governing stationary states under equilibrium (3.1E) and nonequilibrium (3.1N) boundary conditions are particular cases of the canonical cusp manifold (4.2). This is the manifold of critical points of the potential (4.1). Therefore, with an appropriate choice of the control parameters, we can associate a potential function to the Dicke model under both equilibrium and nonequilibrium conditions. Specifically, these potentials are the integrals of Eqs. (3.1E) and (3.1N),

$$\text{E: } V(\mu_e) = \omega\mu_e^2 - \beta^{-1}\ln\cosh\beta\theta + \text{const}\,,$$
$$\theta^2 = (\tfrac{1}{2}\epsilon)^2 + \lambda^2(\mu_e + \alpha)^2\,, \tag{5.1}$$

$$\text{N: } V(\mu_s) = \tfrac{1}{4}\mu_s^4 + \tfrac{2}{3}\mu_s^3\alpha + [\tfrac{1}{2}\alpha^2 + (\gamma_\parallel\gamma_\perp/8\lambda^2)]\mu_s^2 - (\gamma_\parallel\sigma_\infty/8\kappa)(\mu_s + \alpha)^2\,. \tag{5.2}$$

If the constant term in Eq. (5.1) is chosen equal to $-kT\ln 2$, the minimum value of $V(\mu_e)$ is the free-energy per particle[4,13] in the thermodynamic limit ($N \to \infty$). For $\alpha = 0$, the potential $V(\mu_s)$ [Eq. (5.2)] has been used to describe the operation of a single-mode laser[2,3,12] and the thermodynamics of a single-mode laser in the presence of an injected external field.[3]

VI. OPTICAL BISTABILITY

A special case of the nonequilibrium behavior discussed in Sec. IV has been investigated recently under the name of optical bistability.[5,7,9]

When a coherent external field propagates through a cavity containing a collection of resonant two-level systems, the transmitted intensity, under appropriate conditions, can exhibit a discontinuous dependence on the incident intensity. Bonifacio and Lugiato[7] have shown that the steady-state behavior of the transmitted-field amplitude $z(=\mu_s + \alpha = x + \frac{1}{3}\alpha)$ can be described by the cubic equation

$$y = 2cz/(1 + z^2) + z\,, \tag{6.1}$$

where y is proportional to the incident amplitude. The parameter c (which is proportional to the number of atoms in the resonant cavity) is the ratio of the superfluorescent atomic decay rate γ_R to the transverse relaxation rate $\gamma_\perp$ (more precisely, $c = \gamma_R/2\gamma_\perp$). For $c < 4$, the transmitted field amplitude varies monotonically with y. For $c > 4$, instead, the system exhibits bistable behavior, hysteresis, discontinuous jumps, and divergence.

We specialize the remarks of Sec. IV to discuss optical bistability in terms of the manifold of stationary states (4.2) and the control parameters (4.3N). Let $\gamma_R = \lambda^2/\kappa$ and $c = \gamma_R/2\gamma_\perp$. The control parameters in Eq. (4.3N) take the form

$$A = \frac{\alpha^2}{3} - \frac{\gamma_\perp}{2\kappa}\left(1 + \frac{1}{2c}\right)\,,$$
$$B = \frac{2\alpha^3}{27} - \frac{\alpha}{3}\frac{\gamma_\perp}{2\kappa}\left(1 + \frac{1}{2c}\right) + \frac{\gamma_\perp}{2\kappa}\frac{\alpha}{2c}\,, \tag{6.2}$$

where we have set $\sigma_\infty = -1$. All the trajectories in control-parameter space (see Fig. 3) for a fixed value of c and α increasing from zero start with $B = 0$ and negative A. Some trajectories move to the right of the origin, while others move to the left. In the first case, the stationary values of z move continuously onto the upper sheet and no phase transition occurs. If a trajectory curves to the left of the origin the stationary points move

continuously down to the lower sheet and remain there until the right fold line is reached. At this point, the system jumps suddenly onto the upper sheet. Clearly, the necessary condition for a phase transition and bistable behavior is $B<0$ when $A=0$. From Eq. (6.2), we find that this is satisfied if $c>4$, in agreement with the result of Bonifacio and Lugiato.

If at this point α decreases, z reverses its motion on the upper sheet, remains there until it crosses the left fold line, and then jumps to the lower sheet discontinuously. The trajectory of stationary points which passes through $A=B=0$ as α increases corresponds to the condition $c=4$. This trajectory separates two physically distinct regimes: for $c<4$, uncorrelated atomic motion prevails, while, for $c>4$, the atomic system exhibits correlation and cooperativity even in the steady state, provided the input field is maintained below the threshold value for a discontinuous transition from the lower to the upper sheet.

VII. DENSITY OPERATORS

The physical state of a system is completely characterized by the density operator ρ. Under the mean-field assumptions leading from Eq. (2.4) to Eq. (2.6), the density operator factors into the direct product of two reduced-density operators ($\rho=\rho_F\otimes\rho_A$), ρ_F describing the field subsystem alone and ρ_A the atomic subsystem. This factorization assumption is a good approximation except in the neighborhood of the critical point itself.

To the field subsystem, the atomic subsystem looks like a classical driving source (current). A classical current maps field coherent states into coherent states under a unitary transformation $U(\epsilon)$, i.e., $|\mathrm{coh}\rangle\to|\mathrm{coh}\rangle'=U(\epsilon)|\mathrm{coh}\rangle$.[20] In particular, it maps density operators into density operators according to the transformation $\rho_F\to\rho_F'=U(\epsilon)\rho_F U^\dagger(\epsilon)$. If the field system is originally in the ground state or in some pure state, or, more generally, if it is described by a density operator which is the exponential of a Hermitian linear superposition of the creation, annihilation, and photon-number operators, then it will evolve into a state described by a density operator with the same general structure. This extension of the semiclassical theorem from generalized coherent states[13] to density operators is easily proven by group-theoretical methods. This is done in Appendix A.

Entirely analogous considerations hold for the reduced-atomic-density operator ρ_A. In its most general form under the mean-field approximation, ρ_A is the exponential of a Hermitian linear superposition of the atomic operators $\sigma_j^z, \sigma_j^\pm$.

In the following two subsections we construct the reduced-density operators ρ_F, ρ_A. These operators "factor" into a "geometric" part and a "physical" part:

$$\rho_{F\text{ or }A}=[\rho_{F\text{ or }A}(\mathrm{geometric})]^M . \tag{7.1}$$

The operators $\rho_{F\text{ or }A}(\mathrm{geometric})$ exist in a one-to-one correspondence with points on the cusp manifold. The real number M is completely determined by the system noise (fluctuations). In Sec. VII D, we consider an application.

A. Reduced-field-density operator

From the preceding discussion it follows that, under the stated conditions, the most general form of the reduced-field-density operator is

$$\rho_F=\exp(Ma^\dagger a+Ra^\dagger+La) . \tag{7.2}$$

Here and below we work with un-normalized density operators. A very useful generating function for moments of field operators is the expectation value of the operator $\theta=\exp(\eta a^\dagger a+\rho a^\dagger+\lambda a)$, where η, ρ, and λ are arbitrary parameters. This can be calculated from simple 3×3 matrix multiplication and a few deep theorems from the theory of Lie groups[21]:

$$\begin{aligned}\langle\theta\rangle&=\frac{\mathrm{Tr}\rho_F\theta}{\mathrm{Tr}\rho_F}\\&=\frac{1-e^M}{1-e^{M+\eta}}\exp\left[-\frac{\lambda\rho}{\eta}+\left(\frac{L}{M}-\frac{\lambda}{\eta}\right)\left(\frac{R}{M}-\frac{\rho}{\eta}\right)\right.\\&\qquad\left.\times\frac{(e^M-1)(e^\eta-1)}{e^{M+\eta}-1}\right] .\end{aligned} \tag{7.3}$$

From Eq. (7.3) one easily determines

$$\begin{aligned}&\langle a\rangle=-R/N,\quad\langle a^\dagger\rangle=-L/N\\&\langle a^\dagger a\rangle=\frac{e^M}{1-e^M}+\langle a^\dagger\rangle\langle a\rangle=\mathfrak{N}+\mathcal{S} .\end{aligned} \tag{7.4}$$

Thus, we can write the reduced-density operator ρ_F as

$$\begin{aligned}&\rho_F=[\rho_F(\mathrm{cusp})]^M ,\\&\rho_F(\mathrm{cusp})=\exp(a^\dagger a-\langle a^\dagger\rangle a-\langle a\rangle a^\dagger) ,\end{aligned} \tag{7.5}$$

where

$$\frac{e^M}{1-e^M}=\mathfrak{N}=\langle a^\dagger a\rangle-\langle a^\dagger\rangle\langle a\rangle .$$

The operator $\rho_F(\mathrm{cusp})$ is completely determined by a point x on the cusp manifold through the correspondence

$$\begin{aligned}&\mathcal{S}=|\langle a\rangle|^2=|\mu|^2N ,\\&\mu=x-K\alpha ,\end{aligned}$$

where $K=1$ under equilibrium boundary conditions, and $K=\frac{2}{3}$ under nonequilibrium conditions. The real number M characterizes the noise level.

B. Reduced-atomic-density operator

Under the long-wavelength approximation, each atom sees the same driving field. Under the mean-field approximation, each atom is equivalent to all the others. Thus the N-atom density operator factors into the product of N identical single-atom density operators

$$\rho_A = \prod_{i=1}^{N} \otimes \rho_i \,, \qquad \rho_i = \exp(\tfrac{1}{2} M' \sigma_i^z + R' \sigma_i^+ + L' \sigma_i^-). \tag{7.6}$$

In the following development, we drop the subscript i when convenient. If we proceed as in the field case, we find

$$\rho = [\rho(\text{cusp})]^{M'},$$

where

$$\rho(\text{cusp}) = \exp(\langle\sigma^z\rangle \tfrac{1}{2}\sigma^z + \langle\sigma^+\rangle\sigma^- + \langle\sigma^-\rangle\sigma^+),$$
$$M' = |\sigma|^{-1}\tanh^{-1}2|\sigma|, \tag{7.7}$$
$$|\sigma|^2 = (\tfrac{1}{2}\langle\sigma^z\rangle)^2 + \langle\sigma^+\rangle\langle\sigma^-\rangle, \quad 0 \le |\sigma| \le \tfrac{1}{2}.$$

The expectation values $\langle\sigma^z\rangle, \langle\sigma^\pm\rangle$ are related to the coordinate x on the cusp manifold through Eq. (2.6) together with the appropriate boundary conditions. The real number M' gives a measure of the atomic noise. The parameter $|\sigma|$ ranges from zero for completely disordered systems to $\frac{1}{2}$ for systems in a pure atomic coherent state.[22]

C. Boundary conditions

Equilibrium. Cases i and ii

Under equilibrium conditions we have $\mathfrak{N} = (e^{-M}-1)^{-1} = (e^{\beta\omega}-1)^{-1}$ and $-M = \omega/kT$. Then we can write

$$\rho_F = \exp[-\beta H_1(\nu)], \qquad \rho_{A,i} = \exp[-\beta H_2(\mu)], \tag{7.8}$$

where

$$H_1(\nu) = \mathrm{Tr}(\rho_A H_D)/\mathrm{Tr}\rho_A, \qquad H_2(\mu) = \mathrm{Tr}(\rho_F H_D)\mathrm{Tr}\rho_F. \tag{7.9}$$

The Hamiltonian $H_1(\nu)$ is obtained from H_D by replacing the atomic operators $\sigma^z, \sigma^\pm$ by their mean-field expectation values. The Hamiltonian $H_2(\mu)$ is obtained by replacing the field operators by their mean-field values $\langle a\rangle = \mu\sqrt{N}$.[13,14,18]

Nonequilibrium. Cases i and ii

Under nonequilibrium conditions, we have

$$\rho_F(\text{cusp}) = \exp[a^\dagger a - (x - \tfrac{2}{3}\alpha)\sqrt{N}(a^\dagger + a)],$$
$$-M = \ln(1 + \mathfrak{N}^{-1}), \tag{7.10}$$
$$\rho_{A,i}(\text{cusp}) = \exp\left[\sigma_s \tfrac{1}{2}\sigma^z + \frac{i\kappa}{\lambda}(x - \tfrac{2}{3}\alpha)(\sigma^+ - \sigma^-)\right],$$
$$\sigma_s = \sigma_\infty - 4(\kappa/\gamma_\parallel)(x + \tfrac{1}{3}\alpha)(x - \tfrac{2}{3}\alpha),$$

with M' determined from Eq. (7.7).

D. An application

In photon-counting experiments, the probability that k photons are absorbed when the system is in an initial state $|i\rangle$ is[10]

$$p(k) = \sum_f |\langle f|a^k|i\rangle|^2. \tag{7.11}$$

When the sum of final states is carried out, Eq. (7.11) becomes

$$p(k) = \langle i|(a^\dagger)^k a^k|i\rangle. \tag{7.12}$$

In a realistic experimental situation, the initial state of the field is not reproducible with certainty. If a sum is now carried out in Eq. (7.12) over all possible initial states, each element of the sum being weighted according to its relative probability, the measurable probability of absorbing k photons is given by

$$p(k) = \mathrm{Tr}(\rho_F (a^\dagger)^k a^k)/\mathrm{Tr}\rho_F = \langle (a^\dagger)^k a^k\rangle. \tag{7.13}$$

Observe that

$$(a^\dagger)^k a^k = a^\dagger a(a^\dagger a - 1)\cdots(a^\dagger a - k + 1).$$

The generating function $\langle \exp\eta a^\dagger a\rangle$ is easily determined from Eq. (7.3):

$$\langle \exp\eta a^\dagger a\rangle = \frac{1 - e^M}{1 - e^{M+\eta}} \exp\left(\frac{LR}{M^2}\frac{(e^M - 1)(e^\eta - 1)}{e^{M+\eta} - 1}\right). \tag{7.14}$$

This is a convenient generating function both for moments and for factorial moments of the number operator, since

$$\left(\frac{\partial}{\partial\eta}\right)^k \langle \exp\eta a^\dagger a\rangle|_{\eta=0} = \langle (a^\dagger a)^k\rangle \tag{7.15a}$$

$$\left(\frac{\partial}{\partial e^\eta}\right)^k \langle \exp\eta a^\dagger a\rangle|_{\eta=0} = \langle a^\dagger a(a^\dagger a - 1)\cdots(a^\dagger a - k + 1)\rangle = \langle (a^\dagger)^k a^k\rangle. \tag{7.15b}$$

In particular, the first moment is given by Eq. (6.4). The generating function (7.14) can be expressed explicitly in terms of the signal $\mathcal{S} = LR/M^2$

and the noise parameters $\mathfrak{N} = e^M/(1-e^M)$ as follows:

$$\langle \exp\eta a^\dagger a\rangle = [1-\mathfrak{N}(e^\eta-1)]^{-1}\exp\left\{\frac{\mathcal{S}(e^\eta-1)}{1-\mathfrak{N}(e^\eta-1)}\right\}. \tag{7.16}$$

Equation (7.16) can be recognized as the generating function for Laguerre polynomials[23]

$$(1+z)^{-1}\exp\left(-\frac{yz}{1-z}\right) = \sum_{k=0}^{\infty} L_k(y)z^k, \quad |z|<1 \tag{7.17}$$

with $z = \mathfrak{N}(e^\eta-1)$, $-y = \mathcal{S}/\mathfrak{N}$

The moments $\langle (a^\dagger a)^k\rangle$ can be computed from Eq. (7.16) with result

$$\langle (a^\dagger a)^k\rangle = \sum_{j=0}^{k} L_j(-\mathcal{S}/\mathfrak{N})\mathfrak{N}^j \frac{d^k}{d\eta^k}(e^\eta-1)^j\big|_{\eta=0}. \tag{7.18}$$

The factorial moments $\langle (a^\dagger)^k a^k\rangle$ can also be obtained from the generating function (7.16) upon expanding the latter in power of e^η. This is done by writing

$$\frac{1}{1-\mathfrak{N}(e^\eta-1)} = \frac{1}{1+\mathfrak{N}}\,\frac{1}{1-[\mathfrak{N}/(1+\mathfrak{N})]e^\eta},$$
$$\frac{\mathcal{S}(e^\eta-1)}{1-\mathfrak{N}(e^\eta-1)} = -\frac{\mathcal{S}}{1+\mathfrak{N}}\left(1-\frac{e^\eta/(1+\mathfrak{N})}{1-[\mathfrak{N}/(1+\mathfrak{N})]e^\eta}\right). \tag{7.19}$$

The result of the simple calculation is

$$\langle (a^\dagger)^k a^k\rangle = \frac{1}{1+\mathfrak{N}}\left(\frac{\mathfrak{N}}{1+\mathfrak{N}}\right)^k \times L_k\left(-\frac{\mathcal{S}}{\mathfrak{N}(1+\mathfrak{N})}\right)e^{-\mathcal{S}/(1+\mathfrak{N})}. \tag{7.20}$$

It is worth emphasizing the signal $\mathcal{S}$ determines the point x on the cusp manifold through the relation $\mathcal{S} = (x-K\alpha)^2N$ (N=the number of atoms). The expression $\langle a^\dagger a\rangle - \langle a^\dagger\rangle\langle a\rangle$ determines the noise.

VIII. STABILITY

We discuss three types of stability. In Secs. VIII A and VIII B, we assume $\mu = \langle a\rangle/\sqrt{N}$ to be real. The reason for this assumption and the conditions under which it is valid are considered in Sec. VIII C.

A. Static stability

All points on the stationary manifold in the single-valued region outside the cusp-shaped region in Figs. 1, 2, and 3 represent stable physical systems. When the control parameters take values inside this region, points on the upper and lower sheets represent stable or metastable systems; points on the middle sheet represent unstable stationary states. These remarks hold for both equilibrium and nonequilibrium boundary conditions.

B. Dynamical stability

The dynamical-stability properties of the time-dependent set of equations (2.6) are determined by linearizing these equations about the stationary values and investigating the nature of the roots of the resulting eigenvalue equations. We illustrate the procedure in the case in which the decay rate of the field variable μ is the largest of all the decay rates in Eqs. (2.6). In this case, the field variable can be eliminated adiabatically leading to the coupled linear equations

$$i\left(\frac{d}{dt}+\gamma_\perp\right)\delta\nu = -\frac{\lambda^2\sigma_s}{i\kappa}\,\delta\nu - \lambda(\mu_s+\alpha)\delta\sigma,$$
$$i\left(\frac{d}{dt}+\gamma_\parallel\right)\delta\sigma = \frac{2\lambda^2}{i\kappa}(\nu_s\,\delta\nu^* + \nu_s^*\delta\nu) + 2(\mu_s+\alpha)[(\lambda\delta\nu)^* - \lambda\delta\nu], \tag{8.1}$$

where $\delta\nu = \nu-\nu_s$, $\delta\sigma = \sigma-\sigma_s$.

The unstable equilibrium points on the middle sheet are saddle nodes. The equilibria on the lower sheet are stable nodes. The equilibria on the upper sheet are stable foci far from the left-hand fold line. However, as the equilibrium point on the upper sheet approaches the fold line, mode softening occurs, and the stable focus becomes a stable node. Critical slowing down then occurs as the equilibrium point moves yet closer to the fold line.

C. Structural stability

We first investigate the consequences of relaxing the assumption that $\langle a\rangle/\sqrt{N}$ is real. Under these conditions, the potentials (5.1) and (5.2) governing the system depend on the two real variables $\mathrm{Re}\mu$, $\mathrm{Im}\mu$. Therefore, the static stability properties of the system are governed by the signs of the eigenvalues of the matrix of mixed second partial derivatives of the potential with respect to the real and imaginary parts of μ.

The inertia of this matrix is (+, +) in the single-sheeted region outside the cusp-shaped domain of the control plane. For $\alpha = 0$ both potentials are $U(1)$ invariant, or cylindrically symmetric. This is a reflection of the gauge invariance of the Dicke Hamiltonian with $\alpha = 0$.[6,14] Above threshold, the potential has the shape of a sombrero.[24] For $\alpha = 0$, the inertia is (+, 0) on the upper and lower sheets, with $|\mu| \neq 0$, and (−, −) on the central sheet, with $\mu = 0$. On the upper sheet, for $B < 0$, and on the lower sheet, for $B > 0$, the inertia is (−, −).[14] These considerations are valid under both boundary conditions.

For μ real, the inaccessible region of the cusp

manifold is only the central sheet. For $A>0$, the potential $V(x;A,B)$, with x real, looks like a cross-section of the sombrero through its axis of symmetry. Changing α from positive to negative tips the potential from one side to the other. As α is made smaller, the stable state becomes metastable and finally unstable when the barrier between it and the stable state vanishes.

For μ complex, the potential surface looks like the whole sombrero. Changing α from positive to negative tips the sombrero from one side to the other. As α passes through zero, the values of the potential on the rim are equal. Changing α slightly causes the system state to "roll around the rim" to the new minimum. The potential has no metastable states. It is for this reason that the middle sheet, with the left side of the upper sheet ($A>0$, $B<0$), and the right side of the lower sheet ($A>0$, $B>0$) are inaccessible when $\langle a\rangle/\sqrt{N}$ is complex.

Lack of metastable states for μ complex forbids the occurrence of first-order transitions. Since they do occur,[9] a physical mechanism must be present to break the gauge invariance when $\alpha=0$. It is known[14,18] that the presence of either the counter-rotating terms $a^\dagger\sigma_j^+$, a σ_j^- or the $\vec{A}\cdot\vec{A}$ term $K(a^\dagger-a)^2$ breaks the gauge invariance and produces a "rigid" Hamiltonian.[6]

We estimate the importance of the nonresonant counter-rotating terms relative to the resonant interaction terms to be given approximately by $|[1+i\tau(\epsilon-\omega)]/[1+i\tau(\epsilon+\omega)]|$, where ϵ is the atomic-level spacing and τ the Wigner-Weisskopf decay time. In the optical regime, and for resonant interaction, the nonresonant terms are unimportant. Thus, it is reasonable to conclude that the $\vec{A}\cdot\vec{A}$ is responsible for breaking the gauge invariance. The inclusion of this term in the mathematical analysis of Secs. II and III does not cause any major modifications in the absence of counter-rotating terms, except that $\langle a\rangle/\sqrt{N}$ is no longer complex but real.

With this justification for the assumption that $\langle a\rangle$ is real when α is real, we turn to a discussion of the structural stability of the equations describing the stationary states of the Hamiltonian (2.1). The stationary manifolds (4.3E) and (4.3N) both have the form (4.2). In the equilibrium case, A and B are invertible functions of the physical control parameters β and α. In the nonequilibrium case, they are invertible functions of the physical controls σ_∞ and α. Since (4.1) is a universal unfolding[15,16,25] of x^4, the potentials (4.3E) and (4.3N) are both structurally stable. The dynamical system (2.6) is, therefore, also structurally stable.

For $\alpha=0$, the Eqs. (4.3E) and (4.3N) and the dynamical system (2.6) are not structurally stable. This implies that qualitatively new effects can be expected under small perturbations, such as applied external fields. Since these equations are structurally stable with the parameter $\alpha\neq 0$, no qualitatively new steady-state behavior will be observed when further perturbations (classical currents, magnetic fields, etc.) are introduced.[26]

Additional types of dissipative structures can be found at very high pumping levels if order parameters for time-periodic and/or space-periodic behavior are introduced in Eqs. (2.6).[27]

IX. SUMMARY AND CONCLUSIONS

The Langevin equations were derived for the interacting system consisting of a single field mode and N identical two-level atoms (Dicke model) including the effects of an external field and heat baths. Under the mean-field approximation, the density operator factors into the product of reduced density operators. The Langevin equations reduce to a system of coupled nonlinear equations for the operator expectation values $\langle a\rangle$, $\langle\sigma^-\rangle$, $\langle\sigma^z\rangle$, $\langle a^\dagger a\rangle$.

The stationary states for this system of coupled nonlinear equations were determined under both equilibrium and nonequilibrium boundary conditions. This was done by transforming the system of equations to a single nonlinear equation for the operator expectation value $\langle a\rangle$. Under both types of boundary conditions, the resulting equation was found to be essentially a cubic. As a result, the manifold of stationary states was immediately identified with the "cusp catastrophe."

In the absence of external fields ($\alpha=0$), the system undergoes a Ginzburg-Landau-type second-order phase transition as a function of increasing control parameters $\beta(E)$ or $\sigma_\infty(N)$ provided

$$\begin{aligned} &\text{E:}\quad \lambda^2/(\mathrm{Re}\epsilon')(\mathrm{Re}\omega')>1\,,\\ &\text{N:}\quad \lambda^2/(\mathrm{Im}\epsilon')(\mathrm{Im}\omega')>1\,, \end{aligned} \tag{9.1}$$

where

$$\epsilon'=\epsilon+i\gamma_\perp\,,$$

$$\omega'=\omega+i\kappa\,.$$

The Ginzburg-Landau phase transition (bifurcation) is structurally unstable against small perturbations. Under both equilibrium and nonequilibrium boundary conditions, for fixed $\alpha>0$, the system state passes continuously onto the upper sheet in Fig. 1, and no phase transition occurs. Under equilibrium conditions, if the temperature is held below a critical value and the field α is varied from a positive to a sufficiently negative value, a first-order phase transition occurs (Fig.

2). Under nonequilibrium conditions, if the population inversion is held below threshold and the field is made sufficiently strong, a first-order phase transition can occur if $\lambda^2(-\sigma_\infty)/8\gamma_\perp\kappa > 1$. In both cases, hysteresis, discontinuity, and divergence occur.

Potentials governing the system under both equilibrium and nonequilibrium conditions were easily obtained by integrating the Eqs. (3.1) for the stationary manifold. In the equilibrium case, the potential (5.1) is just the free energy. In the nonequilibrium case the potential (for $\alpha = 0$) is just the "laser free energy."

The connection between the results of our discussion for the nonequilibrium case and the conditions for the occurrence of optical bistability have been made explicit.

The reduced density operators were computed in the mean-field approximation. In all cases (E or N; ρ_F or ρ_A; $\alpha = 0$ or $\alpha \neq 0$) the reduced operators "factor" according to $\rho = [\rho(\text{geometry})]^{M(\text{physics})}$. The operator ρ(geometry) depends only on the particular point x in the cusp manifold which represents the system state. The real number M(physics) depends only on the physics of the system. The Glauber photocount-probability distribution function was derived, and it was determined that the system signal fixes ρ(geometry), while the system noise fixes M(physics).

The identification of points on the cusp manifold with density operators $\rho_F \otimes \rho_A$ for systems subject to both equilibrium and nonequilibrium boundary conditions allows the possibility of an "analytic continuation" from one set of boundary conditions to the other. The analytic continuation is not in the usual complex variable sense, despite the suggestion of Eq. (9.1). It is, rather, in the sense of real differential geometry. The cusp manifold (4.2) is analytic; it is only its projection down to the control plane which is not.[28] The identification of density operators with the cusp, and of the stationary manifolds (4.3E) and (4.3N) with the cusp, allows a comparison of photocount experiments performed under the two different types of boundary conditions.

The static stability of the stationary manifolds (3.1), the dynamic stability of the Langevin equations (2.6) and the structural stability of the Hamiltonian (2.2) were discussed. Without the external field all three systems are structurally unstable. However, only one additional (nondegenerate) dimension is required to produce structurally stable stationary systems by Thom's theorem.[8] The important result follows that no new quasistationary effects remain to be discovered by considering additional perturbations of (2.2). The only effect any additional perturbations may have is to enrich the spectrum of possible trajectories in the space of control parameters (A, B). Those trajectories which cross the bifurcation set (fold lines) produce first-order phase transitions.

The physical implications of Eq. (3.1) were discussed in Sec. VIII. In the Appendix, we have extended the semiclassical theorem from generalized coherent states to Gibbs states.

Successful though the Dicke model[1] has been, it represents, in some sense, a history of missed opportunities. When the Langevin equations were first derived,[2] it was assumed that the equilibrium expectation values $\langle a \rangle_e, \langle \sigma^- \rangle_e$ were zero which is indeed true for nonequilibrium boundary conditions. Had this assumption been relaxed, and nonzero stationary solutions sought, the equilibrium phase transition[3] would have been discovered much earlier. If Thom's theorem[8] and the mathematical theory of unfolding[25] had been available, it would have been realized that the second-order phase transition under both equilibrium and nonequilibrium boundary conditions forces a pleat into the manifold of stationary states (Fig. 1). This pleat guarantees the presence of first-order transitions provided only that appropriate trajectories in control-parameter space are followed. In addition, since the universal unfolding of the Ginzburg-Landau potential requires only one additional parameter [B in Eq. (4.1)], the complete structurally stable behavior of the Dicke Hamiltonian would have been studied by introducing only one type of external perturbation. As it was, each type of behavior was analyzed separately and independently according to

	External field	
	i	ii
Boundary conditions	$=0$	$\neq 0$
E: equilibrium	Ref. (4)	(6)
N: nonequilibrium	(2)	(7)

(9.2)

ACKNOWLEDGMENTS

One of us (L.M.N.) thanks Prof. R. Bonifacio and Prof. L. A. Lugiato (Milan) for making their results (Ref. 7) available prior to publication. The other thanks Prof. Harry Thomas (Basel) for useful discussions on the relation between photocount experiments carried out under both equilibrium and nonequilibrium conditions. He also thanks Dr. T. Poston (Geneva) for very enlightening discussions on the subject of "elementary catastrophe theory." This research was supported in part by the Office of Naval Research under Contract No. N0014-76-C-1082.

APPENDIX

We extend the semiclassical theorem from coherent states to Gibbs states. Although the semiclassical theorem for generalized coherent states has been proven already,[11] the proof is not easily accessible; so we prove this theorem first.

There are four required structures for the construction of generalized coherent states.[11] (a) A real[29] Lie group G with real Lie algebra $\mathcal{G}$ spanned by basis vectors (operators) $X_1, X_2, \ldots, X_n$. (b) An invariant space V^λ which carries a unitary irreducible representation Γ^λ of G. (c) An extremal vector $|\lambda; \text{ext}\rangle$ in V^λ. Such vectors may be found in two distinct but equivalent ways: $|\lambda; \text{ext}\rangle$ is an extremal state if (1) it is annihilated by a solvable subalgebra of the complex extension[29] of $\mathcal{G}$ of maximal dimensions or (2) it is a nondegenerate eigenstate of minimal eigenvalue of some operator in $\mathcal{G}$. (d) A maximal subgroup H_λ of G with the property that it leaves $|\lambda; \text{ext}\rangle$ fixed up to a phase factor

$$h|\lambda; \text{ext}\rangle = |\lambda; \text{ext}\rangle e^{i\Phi(h)}, \quad h \in H_\lambda . \tag{A1}$$

For an arbitrary group element $g \in G$, there is the unique decomposition $g = ch$ with $h \in H_\lambda$ and the group operation c contained in the space of coset representatives, $c \in G/H_\lambda$. Generalized coherent states $|\lambda; c\rangle$ are defined by

$$\begin{aligned} g|\lambda; \text{ext}\rangle &= c(h|\lambda; \text{ext}\rangle) = c|\lambda; \text{ext}\rangle e^{i\Phi(h)} \\ &\equiv |\lambda; c\rangle e^{i\Phi(h)}. \end{aligned} \tag{A2}$$

These states exist in one-one correspondence with points in the space G/H_λ. Their properties have been studied extensively.[10,30,31]

For a single electromagnetic field mode, $G = H(4)$, V^λ is the Fock space, and a possible extremal state is $|\text{ext}\rangle = |0\rangle$, the state with no photons.[20] For two-level atoms, $G = \text{SU}(2)$, V^λ carries a $2j+1$-dimensional irreducible representation of SU(2), possible extremal states are $|j; \text{ext}\rangle = |j, j\rangle$ or $|j; -j\rangle$, and $H_j = \text{U}(1)$.[22]

For the semiclassical theorem to follow, we assume a physical system to be governed by the Hamiltonian

$$H = \sum_{k=1}^{\eta} h_k X_k , \tag{A3}$$

where h_k may be time-dependent functions, the sum is Hermitian, the X_k span $\mathcal{G}$, and H acts in V^λ. A convenient extremal state in V^λ is the nondegenerate ground state of H. The time evolution of the system under (A3) is given by the unitary transformation

$$U(t, t_0) = \tau\left(\exp \int_{t_0}^{t} -\frac{i}{\hbar} H(t')dt'\right) . \tag{A4}$$

Here τ is the usual Dyson time-ordering operator. The operator $U(t, t_0)$ is actually a product of infinitesimal unitary transformations, each having the form $\exp[(-i/\hbar)H(t')\Delta t]$. Each of these is a group element in G; the product of all these is also a group element in G. Therefore, $U(t, t_0)$ in (A4) is a time-dependent group element and

$$U(t) = g(t) = c(t)h(t) . \tag{A5}$$

In (A5) we have suppressed the initial time and exploited the coset decomposition.[29]

Semiclassical theorem for coherent states. A system initially in a coherent state, or, in particular, in the ground state, evolves into a coherent state (up to a phase factor) under a Hamiltonian of the form (A3).

Proof. Assume that the system is initially in a coherent state $|\lambda; c_0\rangle$. Then the time evolution is given by (A5) and

$$\begin{aligned} g(t)|\lambda; c_0\rangle &= g(t)c_0|\lambda; \text{ext}\rangle \\ &= c'(t)h'(t)|\lambda; \text{ext}\rangle \\ &= |\lambda; c'(t)\rangle e^{i\Phi(h'(t))} . \end{aligned} \tag{A6}$$

This completes the proof.

The semiclassical theorem may be paraphrased, less precisely, in the form of a selection rule: once a coherent state, always a coherent state.

We turn now to Gibbs states. For systems in thermodynamic equilibrium, these are essentially density operators of the form $\exp(-\beta H)$. However, since we are also dealing with nonequilibrium boundary conditions, we must extend the definition of Gibbs states in order to include this situation as well. Since the Hamiltonian (A3) is a linear combination of the generators X_k of the Lie group G, we define a Gibbs state $E(X) = \exp(\sum \alpha_j X_k)$ to be the exponential of a linear superposition of operators X_k. In short, a Gibbs state is an element in the complex extension G^c of the Lie group G.

Gibbs states are more versatile than coherent states. The Gibbs state for the extremal state of (A3) is

$$E(x_i) = \lim_{\beta \to \infty} e^{-\beta H}/\text{Tr}(e^{-\beta H}) . \tag{A7}$$

The Gibbs state for any other coherent state is

$$\begin{aligned} |\lambda; c\rangle\langle\lambda; c| &= c|\lambda; \text{ext}\rangle\langle\lambda; \text{ext}|c^{-1} \\ &= \lim_{\beta \to \infty} c[e^{-\beta H}/\text{Tr}(e^{-\beta H})]c^{-1} \\ &= \lim_{\beta \to \infty} [e^{-\beta c H c^{-1}}/\text{Tr}(e^{-\beta H})] . \end{aligned} \tag{A8}$$

The denominator in (A8) is unchanged under c because the trace is invariant under similarity transformations. The result (A8) can be simplified further by introducing the regular or adjoint rep-

resentation.[29] The adjoint representation of $X_i \in \mathcal{G}$ is the $(n \times n)$ matrix $\Gamma^A_{kj}(X_i) = c^k_{ij}$, where $[X_i, X_j] = c^k_{ij} X_k$. The adjoint matrix representation of G is the exponential of the adjoint representation of the algebra:

$$\Gamma^A[\exp(\alpha_i X_i)] = \exp[\Gamma^A(\alpha_i X_i)]. \tag{A9}$$

The properties of the adjoint representation of the algebra and of the group are

$$[X_i, X_j] = X_k \Gamma^A_{kj}(X_i), \tag{A10a}$$

$$g X_j g^{-1} = X_k \Gamma^A_{kj}(g). \tag{A10b}$$

Equations (A10a) and (A10b) are the differential and integral forms of the same group-theoretical relation. Equation (A8) can now be simplified using (A10b) with (A3): $cHc^{-1} = X_k \Gamma^A_{kj}(c) h_j$.

Semiclassical theorem for Gibbs states. A system initially in a Gibbs state evolves into a Gibbs state under a Hamiltonian of the form (A3) (once a Gibbs state, always a Gibbs state).

Since the proof is trivial, $[g(t)E(X_i)g^{-1}(t) \in G^e$, Q.E.D.], we prove a more general version of the theorem:

If $f(X_i)$ is an analytic function of the operators $X_1, \ldots, X_n$, then it evolves in the time under (A3) into a function of the same form with covariantly transformed argument.

The simple proof follows:

$$g(t)f(X_i)g^{-1}(t) = f(g(t)X_i g^{-1}(t)) = f[X_j \Gamma^A_{ji}(g(t))]. \tag{A11}$$

Q.E.D.

For a Gibbs state, take $f(X_i) = \exp(\sum \alpha_i X_i)$. The above proof assumes that if the initial state is, for example, an exponential of a quadratic form $f(X_i) = \exp(\alpha_{ij} X_i X_j)$ then it will retain that form for all time: $f(X_i) \to \exp(\alpha_{ij}(t) X_i X_j)$.

We illustrate the usefulness of this theorem by computing the density operator representing the field mode in a statistical superposition of signal and noise.[20] The computation is carried out in two steps.

(a) The vacuum is raised from $T = 0$ to a finite temperature

$$\rho_{\text{vac}} = |0\rangle\langle 0| \to \rho(T) = (1 - e^{-\beta\hbar\omega}) e^{-\beta\hbar\omega a^\dagger a}. \tag{A12}$$

(b) The thermal state is radiated by a classical current which drives the field through a unitary transformation $U(\alpha) = \exp(\alpha a^\dagger - \alpha^* a)$

$$\rho(T) = \rho(T, \alpha) = U(\alpha)[(1 - e^{-\beta\hbar\omega}) e^{-\beta\hbar\omega a^\dagger a}] U(-\alpha)$$
$$= (1 - e^{-\beta\hbar\omega}) \exp[-\beta\hbar\omega (a - \alpha)^\dagger (a - \alpha)]. \tag{A13}$$

In deriving (A13) we have exploited the regular representation of $H(4)$: $U(\alpha) a^\dagger U(-\alpha) = a^\dagger - \alpha^* I$. In computing $\rho(T, \alpha)$, the order of steps (a) and (b) may be reversed.

[1] R. H. Dicke, Phys. Rev. 93, 99 (1954).

[2] H. Haken, *Handbuch der Physik*, Springer-Verlag, Berlin (1970) Vol. XXV/2c; M. Lax, in *Statistical Physics Phase Transitions and Superfluidity, Brandeis Summer Institute, 1966* (Gordon and Breach, New York, 1968), Vol. II, p. 271.

[3] V. De Giorgio and M. O. Scully, Phys. Rev. A 2, 1170 (1970).

[4] K. Hepp and E. H. Lieb, Ann. Phys. (N.Y.) 76, 360 (1973).

[5] S. L. McCall, Phys. Rev. A 9, 1515 (1974).

[6] J. P. Provost, F. Rocca, G. Vallee, and M. Siruge, Physica, 85A, 202 (1976); R. Gilmore, Phys. Lett. A 55, 459 (1976).

[7] R. Bonifacio, L. A. Lugiato, Opt. Commun. 19, 1972 (1976).

[8] R. Thom, Topology 8, 313 (1969).

[9] H. M. Gibbs, S. L. McCall, and T. N. C. Venkatesan, Phys. Rev. Lett. 36, 1135 (1976).

[10] R. J. Glauber, in *Quantum Optics and Proceedings of the Les Houches 1964 Summer School*, edited by C. de Witt *et al.* (Gordon and Breach, New York, 1965), p. 63.

[11] R. Gilmore, Rev. Mex. Fis. 23, 143 (1974).

[12] H. Haken, Rev. Mod. Phys. 47, 67 (1975).

[13] R. Gilmore and C. M. Bowden, Phys. Rev. A 13, 1898 (1976).

[14] R. Gilmore, C. M. Bowden, J. Math. Phys. 17, 1617 (1976).

[15] (a) V. I. Arnol'd, Funct. Anal. Appl. 6, 254 (1972); (b) Russ. Math. Surv. 27(5), 54 (1972).

[16] (a) E. C. Zeeman, Sci. Am. 65, 234 (1976); (b) T. Poston and I. N. Stewart, *Taylor Expansions and Catastrophes* (Pittman, London, 1976); (c) *Catastrophe Theory and How to Apply It* (Pittman, London, 1977); (d) E. C. Zeeman, *Readings in Catastrophe Theory* (Addison-Wesley, Reading, Mass., 1977).

[17] This can be done rigorously because the function $x - \tanh x$ is 3 determinate. See Refs. 15.

[18] R. Gilmore, J. Math. Phys. 18, 17 (1977).

[19] See Fig. 5.7 in Ref. 14(b) or Fig. 2 in Ref. 16.

[20] R. J. Glauber, Phys. Rev. 130, 2529 (1963); 131, 2766 (1963).

[21] R. Gilmore, J. Math. Phys. 15, 2090 (1974).

[22] F. T. Arecchi, E. Courtens, R. Gilmore, and H. Thomas, Phys. Rev. A 6, 2211 (1972).

[23] *Handbook of Mathematical Functions*, edited by M. Abramowitz and I. A. Stegun (Dover, New York, 1970), p. 784.

[24] R. Gilmore and C. M. Bowden, in *Cooperative Effects in Matter and Radiation*, edited by C. M. Bowden, D. W. Howgate, H. R. Robl (Plenum, New York, 1977), p. 335.

[25] J. Mather, Publ. Math. IHES 37, 223 (1969); Adv. Math. 4, 301 (1970); G. Wasserman, *Stability and Unfolding* (Springer-Verlag, Berlin, 1974).

[26] This can be put in a mathematically concise way as

follows: Eq. (2.2) is the structurally stable universal unfolding of the zero-field Dicke model.

[27]Ref. 11, p. 81.

[28]For a succinct statement of this theorem see the work of E. C. Zeeman [in Proceedings of the International Congress on Mathematics, Canadian Mathematical Congress, 1975, p. 533 (unpublished)] or Ref. 15(b), p. 73.

[29]R. Gilmore, *Lie Groups, Lie Algebras, and Some of Their Applications* (Wiley, New York, 1974).

[30]A. M. Perelomov, Commun. Math. Phys. 26, 222 (1972).

[31]R. Gilmore, Ann. Phys. (N.Y.) 74, 391 (1972).